The three-species monomer-monomer model in the reaction-controlled limit

1998 J. Phys. A: Math. Gen. 31 6309

(http://iopscience.iop.org/0305-4470/31/30/001)

J. Phys. A: Math. Gen. **31** (1998) 6309–6318. Printed in the UK PII: S0305-4470(98)89888-0

The three-species monomer–monomer model in the reaction-controlled limit

Kevin E Bassler† and Dana A Browne

Department of Physics and Astronomy, Louisiana State University, Baton Rouge, LA 70803, USA

Received 9 December 1997

Abstract. We study the one-dimensional three-species monomer–monomer reaction model in the reaction-controlled limit using mean-field theory and dynamic Monte Carlo simulations. The phase diagram consists of a reactive steady state bordered by three equivalent adsorbing phases where the surface is saturated with one monomer species. The transitions from the reactive phase are all continuous, while the transitions between adsorbing phases are first order. Bicritical points occur where the reactive phase simultaneously meets two adsorbing phases. The transitions from the reactive to an adsorbing phase show directed percolation critical behaviour, while the universal behaviour at the bicritical points is in the even branching annihilating random walk class. The results are contrasted and compared with previous results for the adsorption-controlled limit of the same model.

1. Introduction

Simple models with continuous phase transitions to an adsorbing steady state where fluctuations are absent are prototypical models for non-equilibrium critical phenomena. These far-from-equilibrium models arise in a variety of contexts ranging from gravity-driven flow through a porous medium to the spread of epidemics and to heterogeneous catalytic reactions.

The critical behaviour at the transition in most of these models belongs to the universality class of directed percolation (DP) [1], which is the simplest model with an adsorbing transition described by an order parameter with no internal symmetry. However, recently a number of models with continuous adsorbing transitions having critical properties not in the DP class have been discovered [2–6]. These models, which include branching annihilating random walks with even numbers of offspring (BAWe) [2], have similar critical properties and thus form a distinct universality class. The distinguishing feature of this class is a conservation modulo 2 of the number of defects [7, 8].

In one-dimensional models, this critical behaviour can be seen in models with two equivalent adsorbing states, where the defects are domain walls between domains of the two different states. The parity conservation law, which requires that the number of defects always remains either even or odd, arises naturally because two domain walls are either created or destroyed each time a domain appears or disappears. The dynamical behaviour of these defects is very rich, showing a variety of scaling behaviours some of which have no analogue in the simpler DP universality class.

† Current address: Department of Physics, University of Houston, Houston, TX 77204, USA.

0305-4470/98/306309+10$19.50

In order to study the role of adsorbing state symmetry in adsorbing phase transitions, we recently introduced the three-species monomer–monomer catalytic reaction model [5]. In this model, three different species of monomers compete for lattice sites through two fundamental dynamical processes: (a) monomer adsorption onto empty lattice sites, and (b) the annihilation reaction of two dissimilar monomers adsorbed on nearest-neighbour lattice sites. We previously studied the one-dimensional version of the model in the adsorption-controlled limit, where the reaction process happens instantaneously. We discovered a phase diagram consisting of three adsorbing phases where the entire lattice is saturated by a single-monomer species, and a reactive phase. The phase transitions between the reactive phase and the saturated phases are continuous and their dynamical critical properties are those of the DP universality class. Phase transitions between saturated phases are first order. Of particular interest are *bicritical* points [9] where two saturated phases meet the reactive phase. At those points the adsorbing state is two-fold degenerate and the dynamical critical properties are those of the BAWe universality class. We also defined and measured three exponents associated with the dynamic behaviour of an interface between domains of the two equivalent adsorbing phases at the bicritical point, and we conjectured that those exponents are universal, characteristic of the BAWe class.

In this paper we investigate the reaction-controlled limit of the model, where the adsorption process happens instantaneously. Using a mean-field analysis and dynamical Monte Carlo simulations, we shall show that all of the qualitative features of the phase diagram remain the same, and that all of the results for critical exponents are consistent with those we found in the adsorption-controlled limit. Most importantly, we confirm our conjecture concerning the universal nature of the interface dynamics exponents we defined previously.

In section 2 we shall present results from mean-field theory for this model. Section 3 discusses our results from dynamic Monte Carlo calculations for the critical exponents of the model, studying the critical behaviour of an isolated defect as well as the interface between two different absorbing phases. Our conclusions are presented in section 4.

2. Mean-field results

The mean-field theory we employ is based on a cluster expansion scheme where the clusters consist of a chain of adjacent sites. For each allowed configuration of a cluster of a given size, we can write down exact rate equations for the time evolution of the number of clusters with that configuration. For our problem, as we shall see below, the equations for a cluster of a given size require knowledge of the number of clusters with one additional size, leading to an infinite chain of equations. The approximation results from truncating the chain of equations at clusters of a given maximum size and replacing expressions for the numbers of larger clusters with approximate forms. This technique, employed by Dickman [10] for studying the ZGB model [11] for CO oxidation, is essentially the same as the Kirkwood superposition approximation used in the theory of liquids. This technique and its generalizations [12] have been used extensively in studies of lattice models.

For our model it is useful to describe a given configuration as having ‘active’ bonds where the two adjacent sites are occupied by monomers of different species, and ‘inactive’ bonds where both sites are occupied by the same species. The configurations can change only where there is an active bond. Thus, the evolution equation for a particular cluster are found by properly enumerating all the ways an active bond could produce the current cluster, and also finding the number of ways the current configuration could disappear because an active bond that the cluster was a part of had changed. For the purposes of deriving the

equations, it is easiest to account separately for the disappearance and the production of active bonds.

If our system has N sites, we define N_A as the number of sites occupied by A monomers. Similarly, the number of AB pairs we denote N_{AB}. For this we treat the number N_{BA} of BA pairs as distinct, although we expect that in the steady state the two are equal. Larger clusters are defined in an obvious fashion.

We begin with the equations for the clusters consisting of one site. The fraction of A sites can change if that site is at either end of an active bond. The exact rate equation for the number of A monomers is

$$\frac{\mathrm{d}N_A}{\mathrm{d}t} = 2p_A(N_{BC} + N_{CB} + N_{AB} + N_{BA} + N_{AC} + N_{CA}) - (N_{AB} + N_{BA} + N_{AC} + N_{CA}). \tag{1}$$

The first term on the right-hand side represents the production of A monomers at active bonds of any kind, the factor of 2 arising from adding monomers at either end of the bond. The second term represents the rate that A monomers disappear because they are part of an active bond that is being updated. The process of picking a site and replacing an A monomer with an A monomer is divided between the two terms. The equations for B and C monomers are found by cyclicly permuting the indices A, B and C.

For the two clusters of pairs of sites, we proceed in a similar fashion. The number of AB clusters decreases every time the bond containing an AB pair is chosen for update, or when the bond to either side of the cluster is active and chosen for update. Production of an AB cluster can proceed by updating an active bond to produce an AB pair. The pair can also be produced by picking the bond to the right of the pair, having the A already present and supplying the B in the update. Similarly one can produce an AB pair by having the B present and updating the bond to the left of the A site to produce the A. The equation for AB pairs is thus

$$\begin{aligned}\frac{\mathrm{d}N_{AB}}{\mathrm{d}t} = {} & p_A p_B(N_{AB} + N_{BA} + N_{AC} + N_{CA} + N_{BC} + N_{CB}) - N_{AB} \\ & + p_B(N_{AAB} + N_{ABA} + N_{AAC} + N_{ACA} + N_{ABC} + N_{ACB}) \\ & - (N_{ABA} + N_{ABC}) + p_A(N_{ABB} + N_{BAB} + N_{ACB} + N_{CAB} + N_{BCB} + N_{CBB}) \\ & - (N_{BAB} + N_{CAB}).\end{aligned} \tag{2}$$

If we were considering a pair occupied by the same monomer, such as an AA pair, the process of selecting the bond occupied by the AA pair and updating it cannot occur, although the other steps in the AB pair equation can occur. The equations for AA pairs is

$$\begin{aligned}\frac{\mathrm{d}N_{AA}}{\mathrm{d}t} = {} & p_A p_A(N_{AB} + N_{BA} + N_{AC} + N_{CA} + N_{BC} + N_{CB}) \\ & + p_A(N_{AAB} + N_{ABA} + N_{AAC} + N_{ACA} + N_{ABC} + N_{ACB}) \\ & - (N_{AAB} + N_{AAC}) + p_A(N_{ABA} + N_{BAA} + N_{ACA} + N_{CAA} + N_{BCA} + N_{CBA}) \\ & - (N_{BAA} + N_{CAA}).\end{aligned} \tag{3}$$

The equations for larger clusters (of size M) are similar in structure to these. We change our notation slightly and denote $N^{(M)}(\alpha_1\alpha_2\ldots\alpha_M)$ as the number of clusters of size M consisting of the configuration $\{\alpha_1\alpha_2\ldots\alpha_M\}$ where each α_i is A, B, or C. The equation of motion for a size M cluster is

$$\frac{\mathrm{d}N^{(M)}(\alpha_1\ldots\alpha_M)}{\mathrm{d}t} = \sum_{i=1}^{M-1} p_{\alpha_i} p_{\alpha_{i+1}} \sum_{\beta\neq\gamma} N^{(M)}(\alpha_1\ldots\alpha_{i-1}\beta\gamma\alpha_{i+1}\ldots\alpha_M)$$

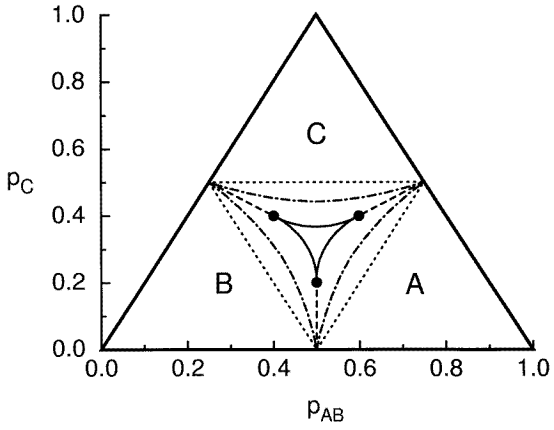

Figure 1. Phase diagram showing three saturated phases (indicated by the letters), and a reactive phase (the unlabelled centre region). Full curves indicate continuous transitions. Broken curves indicate first-order transitions. Bicritical points, shown as full circles, occur where two critical lines meet a first-order line. The site approximation is shown as a dotted curve and the pair approximation as a chain curve.

$$-\sum_{i=1}^{M-1}(1-\delta_{\alpha_i,\alpha_{i+1}})N^{(M)}(\alpha_1\ldots\alpha_M)$$
$$+p_{\alpha_1}\sum_{\beta\neq\gamma}N^{(M+1)}(\beta\gamma\alpha_2\ldots\alpha_M)-\sum_{\beta\neq\alpha_1}N^{(M+1)}(\beta\alpha_1\ldots\alpha_M)$$
$$+p_{\alpha_M}\sum_{\beta\neq\gamma}N^{(M+1)}(\alpha_1\ldots\alpha_{M-1}\beta\gamma)-\sum_{\beta\neq\alpha_M}N^{(M+1)}(\alpha_1\ldots\alpha_M\beta). \quad (4)$$

Despite the simple form of these equations and their close resemblance to equations for two-component models that can be solved exactly [13] and nearly exactly [14], we have not succeeded in solving the set of equations in closed form. As figure 1 shows, the Kirkwood superposition approximation for clusters of size 2 and larger, where $N_{AB} = N_A N_B$, compares poorly with the Monte Carlo results that will be presented below. Improving the approximation to keep the pairs of sites, and using $N_{\alpha\beta\gamma} = N_{\alpha\beta}N_{\beta\gamma}/N_\beta$ improves the agreement somewhat. However, even going to the level of triples of sites, which was sufficient [5] to obtain a qualitative agreement with the Monte Carlo data in the adsorption-controlled limit, failed to produce the coexistence line between the two saturated phases.

The failure of this mean-field approach to produce a realistic position for the bicritical point is linked to the fact that the probability of observing a long cluster of sites all filled with one species, which is approximated in this cluster approach by the probability of a smaller cluster raised to a power, will decay exponentially with the size of the cluster. However, the simulations presented in this paper and in previous work [5] clearly show that at the transitions large domains of each species are present in the steady state, with the fundamental dynamical variables being the domain walls.

Individual large domains do not necessarily cause the mean-field theory to fail, since a similar procedure applied to some monomer annihilation models [13, 14] and cooperative sequential adsorption models [15] yields exact results because the cluster equations close. However, the spatial correlations in those models are very different from ours. The adsorption models have short-ranged correlations, while the monomer annihilation models have long-ranged correlations that result from a simple linear diffusion process. In this model, the long-range correlations are stronger than those produced by simple diffusion, so mean-field theory based on small clusters is not as successful here. This lack of convergence of mean-field models has been seen in other one-dimensional lattice models [12]. There

it was ascribed to having the same phase diagram in all dimensions, which is clearly a restatement of the assumed range of correlations.

3. Simulations

To study the critical properties of the three-species monomer–monomer model we used time-dependent Monte Carlo simulations. This well-established method is a form of 'epidemic' analysis [16] in which the average time evolution of a particular configuration that is very close to an adsorbing state (defect dynamics), or very close to a minimal width interface between two different adsorbing states (interface dynamics), is measured by simulating a large number of independent realizations. Using this technique we located critical and bicritical points and determined the universality classes of the transitions.

In the reaction-controlled limit we are studying, reactions occur only between the nearest-neighbour pairs of dissimilar monomers, that is only between monomers connected by an active bond. Near the continuous phase transitions the number of active bonds is very small. Thus, a traditional Monte Carlo algorithm that picks a bond at random and attempts to react with the monomers is inefficient because most bonds chosen are inactive and no change occurs. Instead, we use a variable time algorithm in which a bond is randomly picked from a list of active bonds, thereby assuring that the reaction will occur. The reacting pair of monomers immediately desorb and then two new monomers immediately adsorb in their places. The species of the new monomers are chosen randomly according to the relative adsorption rates $\{p_\alpha\}$. The time elapsed during a step is $1/n_b(t)$ where $n_b(t)$ is the total number of active bonds at that time. Thus, on average there is one attempted adsorption per bond, or per lattice site, per unit time. We always start with a lattice large enough to ensure that the active region never reaches a boundary; it is effectively an infinite lattice.

During the simulations at the critical point we measured the survival probability $P(t)$, i.e. the probability that the system had not reached an adsorbing state by time t, the average number of active bonds per run $\langle n_b(t)\rangle$, and the average mean-square size of the active region per surviving run $\langle R^2(t)\rangle$. At a continuous adsorbing phase transition as $t \to \infty$ these dynamical quantities show power-law behaviour

$$P(t) \sim t^{-\delta} \qquad \langle n_b(t)\rangle \sim t^{\eta} \qquad \langle R^2(t)\rangle \sim t^{z}. \tag{5}$$

The critical exponents δ, η, and z characterize the universality class of the phase transition.

Precise estimates of the location of the critical point and of the exponents can be made by examining the local slopes of the curves of the measured quantities on a log–log plot. For example, the effective exponent $\delta(t)$ defined as

$$-\delta(t) = \{\ln[P(t)/P(t/b)]/\ln b\} \tag{6}$$

is a numerical approximation of the local slope of the survival probability. In our numerical studies we take $b = 5$. Similar expressions define $\eta(t)$ and $z(t)$. At the critical point, a graph of the local slope versus t^{-1} should extrapolate as $t^{-1} \to 0$ to the critical exponent. The correction to scaling is expected to be linear in t^{-1}†. Away from the critical point, the local slope should curve away from the critical point value as $t^{-1} \to 0$.

The results of our simulations near the phase transition to the C saturated phase at $p_{AB} = 0.5$ are shown in figure 2. These data were extracted from 4×10^5 independent runs of up to 10^4 time steps at each parameter value. We find a critical C monomer adsorption rate of $\tilde{p}_C = 0.3673(1)$, and that the critical exponents are $\delta = 0.155(5)$, $\eta = 0.310(5)$,

† Actually, this statement is known to be true only for directed percolation [20] but it seems to also be true [3] for the BAWe universality class.

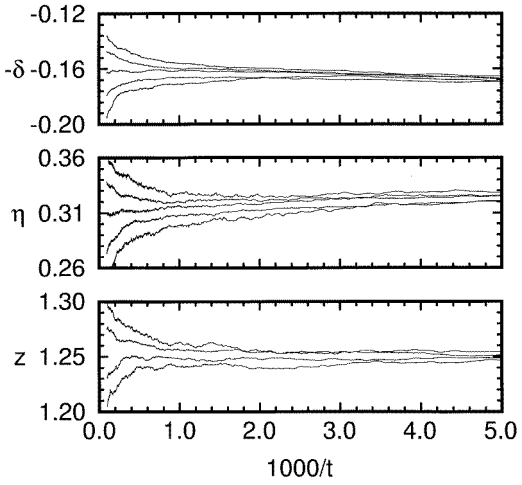

Figure 2. Effective exponents using equation (6) with $b = 5$ for the defect dynamics near the critical point at $p_{AB} = 0.5$ on the curve where the C poisoned phase meets the reactive phase. From top to bottom, the five curves in each panel correspond to $p_C = 0.3671$, 0.3672, 0.3673, 0.3674, and 0.3675, with the middle curve corresponding to the critical point.

and $z = 1.260(10)$. These values are consistent with our expectation that this transition should be in the DP universality class, for which the exponents are [17] $\delta = 0.1596(4)$, $\eta = 0.3137(10)$, and $z = 1.2660(14)$. Our values for the exponents also satisfy the scaling law [16] $4\delta + 2\eta = z$ to within the quoted errors.

The values for all of the exponents we find are slightly lower than those found from series expansion studies [17]. None of the dynamic Monte Carlo studies in the literature examining the critical exponents using local slope analysis include any discussion of how the uncertainties in the exponents are determined. Also, the errors quoted are often considerably smaller than ours even though less data were used. We surmise that the most common error determination involves an eyeball estimate based on the scatter in the local slope curve, or by least-squares fits to the curve. However, error estimates derived from least-squares fits to the local slope cannot be relied on because of the strong correlation between values of the slope at later times on the values at earlier times. Also, there is an uncontrolled systematic error if the critical point value is not known precisely.

We have therefore paid close attention to determining the error. We divided our data into 10 equal sets of 4×10^4 trials. With each data set we independently determined the exponent z by two methods: a least-squares fit to the local slope to extrapolate the local slope to $t^{-1} = 0$, and a linear least-squares fit to plots of $\ln R^2$ versus t^{-1}. The results from each of the 10 independent data sets are combined to give unbiased estimates of the mean and error for the exponent.

In this analysis we found that there was a substantial variation in the value of z found depending on whether data from short times are used. Using the local slope data for times of $t > 1000$, $t > 5000$, and $t > 7500$ for the 10 data sets gave $z = 1.256(1)$, 1.270(5), 1.280(14) respectively. While the short-time data gave a very small error, this is an artefact of using a large amount of data. There is clearly a systematic drift in the value (towards the series expansion value) as the data from shorter times are dropped. Similarly, the least-squares fits to $\ln R^2$ to a form $z \ln t + a/t + b$. gave $z = 1.256(3)$ when fitting data for $t > 1000$ and $z = 1.272(5)$ when using only data for $t > 5000$. Unfortunately the data for $t > 5000$ span only about $\frac{1}{3}$ of a decade in time and so we cannot extrapolate further than that. The longer time data give values closer to that found by series expansion methods, and in both methods of analysis we find statistical errors that are considerably larger than those quoted in other Monte Carlo studies that use less data and shorter times than we

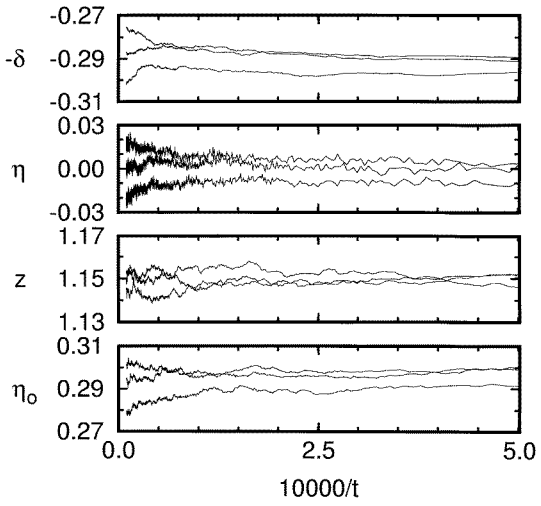

Figure 3. Effective exponents for the defect dynamics near the bicritical point. From bottom to top, the three curves in each panel correspond to $p_C = 0.201$, 0.2015, and 0.202, with the middle curve corresponding to the bicritical point.

adopted here. This exercise points out the potential danger for systematic error in this kind of dynamic Monte Carlo study. The errors we quote above for the exponents are derived from the $t > 1000$ data sets but have been expanded to account for the observed systematic drift we see.

We also studied the dynamics near the bicritical point at $p_{AB} = 0.5$, where the A-saturated and B-saturated phases coexist. Since there are two symmetric saturated phases, the dynamics at the bicritical points are much richer than at critical points. We used two distinct types of epidemic analysis to study the dynamics there.

The first type of epidemic analysis we used to study the bicritical dynamics is analogous to what was described above for the dynamics at the critical point. In this analysis, the average time evolution of a configuration with a single defect in an otherwise adsorbing state was measured. Using an initial condition of a single B monomer in an otherwise A-saturated phase, we measured the same three quantities as before. In addition, we also measured the average number of B monomers present $\langle n_B(t)\rangle$. This quantity is expected to scale in the limit $t \to \infty$ as $\langle n_B(t)\rangle \sim t^{\eta_0}$. The characteristic exponent η_0 is not independent, but is related to the other dynamic exponents by the scaling law [6]

$$\eta_0 = z/2 - \delta. \tag{7}$$

Nevertheless, it is useful to measure η_0 as a numerical check on the other exponents.

The local slope data for the four bicritical defect dynamics exponents are shown in figure 3. These results were calculated using 10^6 runs of up to 10^5 timesteps each. The bicritical point is located at $p_C = p_C^* = 0.2015(5)$, and the exponents are $\delta = 0.285(5)$, $\eta = 0.000(5)$, $z = 1.15(1)$, and $\eta_0 = 0.29(1)$. These values satisfy the scaling law (7) and indicate that the bicritical dynamics falls in the BAWe universality class, for which the exponents are $\delta = 0.285(2)$, $\eta = 0.000(1)$, and $z = 1.141(2)$ [3].

The second type of epidemic analysis that we used to study the dynamics at the bicritical point measures the average time evolution of a minimal width interface between semi-infinite domains of the two different adsorbing states [5]. The simulations are started with a single active bond joining domains of A and B monomers, and the trial is stopped if the interface between the domains collapses back to a single active bond. We thus measure three dynamical quantities analogous to those for the defect dynamics: the probability that at time t the interface has not yet collapsed back to its minimum width, the number of active

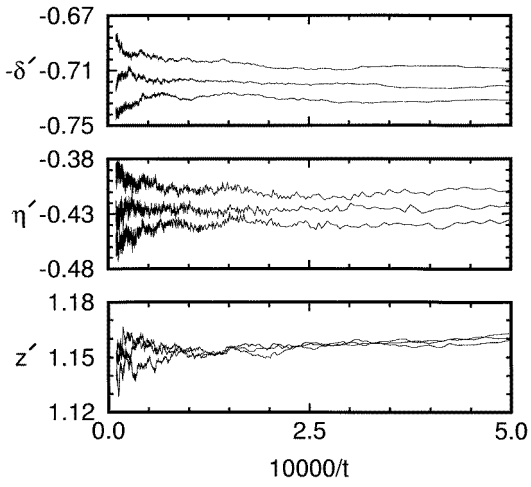

Figure 4. Effective exponents for the interface dynamics near the bicritical point with $b = 5$. From bottom to top, the three curves in each panel correspond to $p_C = 0.201$, 0.2015, and 0.202, with the middle curve corresponding to the bicritical point.

bonds, and the mean square size of the interface. These are characterized at the bicritical point by the exponents δ', η' and z' in analogy with equation (5).

Figure 4 shows the local slope results for these three quantities. The slopes were derived from 10^7 independent runs each lasting up to 10^5 timesteps. From these results we find $\delta' = 0.72(2)$, $\eta' = -0.43(2)$ and $z' = 1.150(15)$. The values of these exponents are consistent with those measured previously [5, 6], and confirm the conjecture [5] that these numbers are universal characteristics of the BAWe dynamics. The value of the dynamic exponent z or z' describing the size of the active region during surviving runs, is the same in both defect and interface dynamics simulations. Furthermore, although the exponents δ and η are different in the two cases, their sums, which govern the time evolution of the number of dissimilar pairs in just the surviving runs, are equal

$$\delta + \eta = \delta' + \eta'.$$

This shows that the critical spreading of the active region for models with two symmetric adsorbing states is universal, independent of whether defect or interface dynamics is being considered. A similar result holds for some one-dimensional systems with infinitely many adsorbing states [18].

4. Summary

We have studied the one-dimensional three-species monomer–monomer reaction model in the reaction-controlled limit. As in our study [5] of this model in the adsorption-controlled limit, the phase diagram consists of a reactive phase and three adsorbing phases where the lattice is saturated with a single species. The phase transitions between the reactive phase and each of the saturated states are continuous, but the transitions between different saturated phases are first order. Bicritical points exist where a first-order line separating two adsorbing phases meets two critical lines separating the reactive phase from each of those phases.

We constructed a mean-field cluster expansion of the model up through triplets of sites. The approximation correctly predicted the existence of the four phases, but failed to predict that the bicritical points occur in the interior of the phase diagram. This result differs from the result of the same analysis for the adsorption-controlled limit of the model. In that

case [5], at the triplet approximation the bicritical points moved off the edge of the phase diagram and the mean-field phase diagram became qualitatively correct. We presume that if quadruples or possibly quintuples of sites are treated in this case, the bicritical points would move off the edge of the phase diagram and the phase diagram would become qualitatively correct.

The dynamic critical behaviour at the transition between the reactive phase and a poisoned phase is in the DP universality class, but at the bicritical points, where there are two equivalent poisoned states, the dynamic critical behaviour is in the BAWe class. Thus, the universality class of the transition changes from DP to BAWe when the symmetry of the adsorbing state is increased from one to two equivalent noiseless states. Furthermore, we have shown that having a symmetry in the adsorbing states introduces a richness into the dynamics that is not possible if there is a unique adsorbing state. In particular, the critical dynamics of the interfaces between two different adsorbing states shows a sensitivity to how the dynamics is defined, and the survival probability of fluctuations in the size of the interface from its smallest value is described by a new universal exponent δ'. However, the critical spreading of the reactive region, be it a defect in a single phase or a domain wall between phases, appears to be insensitive to the choice of initial conditions. This appears to result from the fact that large reactive regions are insensitive to whether the reactive regions are bounded by the same or different saturated phases. We do not expect this result to be true in higher dimensions where the entropy of domain walls can play a role and non-universal critical spreading has been observed in other models [19].

Thus, in conclusion, both the qualitative phase diagram and the universality classes of the critical and bicritical points in the model are equivalent in the reaction- and adsorption-controlled limits of the three-species monomer–monomer reaction model. We confirmed our previous conjecture that the exponents describing the asymptotic behaviour of those dynamics are universal numbers characteristic of the BAWe class. Since these two limits correspond respectively to a zero reaction rate and infinite reaction rate, we predict that any finite reaction rate version of the model will also be equivalent.

Acknowledgments

This work was supported by the National Science Foundation under grant no DMR-9408634. We wish to thank Giovanni Santostasi for assistance in performing some of the simulations in this work.

References

[1] Janssen H K 1981 *Z. Phys.* B **42** 151
[2] Takayasu H and Tretyakov A Y 1992 *Phys. Rev. Lett.* **68** 3060
[3] Jensen I 1994 *Phys. Rev.* E **50** 3623
Zhong D and ben Avraham D 1995 *Phys. Lett.* A **209** 333
[4] Grassberger P, Krause F and von der Twer T 1984 *J. Phys. A: Math. Gen.* **17** L105
Menyhárd N 1994 *J. Phys. A: Math. Gen.* **27** 6139
Menyhárd N and Ódor G 1995 *J. Phys. A: Math. Gen.* **28** 4505
Menyhárd N and Ódor G 1996 *J. Phys. A: Math. Gen.* **29** 7739
Kim M H and Park H 1994 *Phys. Rev. Lett.* **73** 2579
Park H and Park H 1995 *Physica* **221A** 97
Park H, Kim M H and Park H 1995 *Phys. Rev.* E **52** 5664
Hinrichsen H 1997 *Phys. Rev.* E **55** 219
[5] Bassler K E and Browne D A 1996 *Phys. Rev. Lett.* **77** 4094
Bassler K E and Browne D A 1997 *Phys. Rev.* E **55** 5225

[6] Brown K S, Bassler K E and Browne D A 1997 *Phys. Rev.* E **56** 3953
[7] Cardy J and Tauber U C 1996 *Phys. Rev. Lett.* **77** 4780
Cardy J and Tauber U C 1998 *J. Stat. Phys.* **90** 1
[8] Tauber U C, Howard M J and Hinrichsen H 1998 *Phys. Rev. Lett.* **80** 2165
[9] Fisher M E and Nelson D R 1974 *Phys. Rev. Lett.* **32** 1350
[10] Dickman R 1986 *Phys. Rev.* A **34** 4626
[11] Ziff R M, Gulari E and Barshad Y 1986 *Phys. Rev. Lett.* **56** 2553
[12] ben Avraham D and Kohler H 1992 *Phys. Rev.* A **45** 8358
[13] Clément E, Leroux-Hugon P and Sander L M 1991 *Phys. Rev. Lett.* **67** 1661
Krapivsky P L 1992 *Phys. Rev.* A **44** 1067
Krapivsky P L 1992 *J. Phys. A: Math. Gen.* **25** 5831
Evans J W and Ray T R 1993 *Phys. Rev.* E **47** 1018
[14] Sholl D S and Skodje R T 1996 *Phys. Rev.* E **53** 335
[15] Evans J W 1993 *Rev. Mod. Phys.* **65** 1281
[16] Grassberger P and de la Torre A 1979 *Ann. Phys., NY* **122** 373
Grassberger P 1989 *J. Phys. A: Math. Gen.* **22** 3673
[17] Jensen I and Dickman R 1993 *J. Stat. Phys.* **71** 89
[18] Mendes J F F, Dickman R, Henkel M and Marques M C 1994 *J. Phys. A: Math. Gen.* **27** 3019
[19] Vandewalle N and Ausloos M 1995 *Phys. Rev.* E **52** 3447
Dickman R 1996 *Phys. Rev.* E **53** 2223
[20] Grassberger P 1982 *Z. Phys.* B **47** 365